2019 IEEE International Conference on Systems, Man and Cybernetics (SMC)
Bari, Italy. October 6-9, 2019

Quaternion Non-local Total Variation for Color Image Denoising

Xiaoyao Li[1,2], Yicong Zhou[2], and Jing Zhang[1]
[1]*College of Electrical and Information Engineering, Hunan University, Changsha 410082, China*
[2]*Department of Computer and Information Science, University of Macau, Macau 999078, China*
Email: lxyimayday@gmail.com, yicongzhou@umac.mo, zhangj@hnu.edu.cn

***Abstract*— Many existing color image denoising methods process color channels individually and fail to consider their cross-channel correlations. To solve this problem, in this paper, we employ the quaternion representation of the color image and propose a novel Quaternion Non-local Total Variation (QNLTV) model to remove Gaussian noise from color images. We first introduce the coupled quaternion distance to measure the color image patch similarity. Decomposing the color image into brightness and chromaticity components in quaternion domain, we then divide the QNLTV model into two quaternion optimizaiton problems and solve them alternatively. Experiment results show that QNLTV has the significantly better denoising performance than competing methods in terms of visual and quantitative evaluations.**

I. Introduction

The goal of image denoising is to obtain the denoised image $\mathbf{u}$ from the noisy image $\mathbf{f} = \mathbf{u}_0 + \mathbf{n}$, where $\mathbf{u}_0$ is the corresponding clean image and $\mathbf{n}$ is noise such as Gaussian noise with variance σ^2. Because image denoising is an important preprocessing step in image processing, numerous denoising methods have been proposed over the past decades [1]. One of the most well-known denoising techniques to remove Gaussian noise is variation denoising.

As a traditional variation denoising method, the total variation (TV) [2] algorithm was proposed for image denoising in 1992. This algorithm seeks for the optimal solution of a constrained minimization functional comprised of a TV-based regularization term and a fidelity term. Goldstein and Osher proposed a split Bregman method [3] for solving common l_1-regularized problems efficiently. Utilizing this split Bregman framework to TV denoising, they then proposed the split Bregman anisotropic TV (SB-ATV) and the split Bregman isotropic TV (SB-ITV) [3]. In order to preserve more structure information and small scale details, Gilboa et al. [4] replaced the scalar fidelity term in the original TV model with an adaptive one. [5] proposed an efficient and flexible method to solve the generalized vector-valued TV problems, named the vector-valued iteratively reweighted norm (VIRN) algorithm. However, due to the local TV regularization, these TV-based methods frequently produce staircase effects.

After the non-local means (NLM) [6], [7] was proposed by Buades et al. in 2005, many researchers utilized the patch-based non-local idea and proposed many improved TV-based algorithms, such as the non-local TV (NLTV) [8] and the nonlocal version of the generalized relative TV (NLGRTV) [9]. Different from the TV-based methods that use local structure information to develop the optimization models, the non-local versions of TV-based methods take advantages of the relevant image patches to denoise the center noisy patch. Unfortunately, most of the local and non-local TV-based denoising methods deal with each color channel independently and ignore the relationship among color channels. Thus, this leads to unpleasant denoising results.

The purpose of this paper is to propose a new color image denoising method, named the Quaternion Non-local Total Variation (QNLTV) model. QNLTV can process three color channels as a whole by representing a color image pixel as a quaternion. Separating the quaternion representation of color image into brightness and chromaticity componnets, we first introduce the coupled quaternion distance to measure similarity between the color image patches in quaternion domain. We decompose the QNLTV model into two optimization problems. The quaternion split Bregman method is proposed to alternatively optimize these two quaternion optimization models. Experiment results are conducted to demonstrate that QNLTV can effectively remove noise and preserve color image details, and obtain higher SNR and SSIM values than other competing denoising methods.

II. Background

A. Total Variation Model

The TV model proposed by Rudin et al. [2] can be expressed as

$$\mathbf{u} = \arg\min_{\mathbf{u}} \lambda J_{TV}(\mathbf{u}) + \frac{1}{2}\|\mathbf{f} - \mathbf{u}\|_2^2, \tag{1}$$

where $J_{TV}(\mathbf{u})$ is the regularization term and $\frac{1}{2}\|\mathbf{f} - \mathbf{u}\|_2^2$ is the fidelity term. λ is the penalty factor.

There are two popular choices of $J_{TV}(\mathbf{u})$ for TV models. One is the l_2-based isotropic TV defined as [2]

$$J_{TV}(\mathbf{u}) = \|\nabla \mathbf{u}\|_2 = \sqrt{\mathbf{u}_x^2 + \mathbf{u}_y^2}, \tag{2}$$

and the other is l_1-based anisotropic TV defined by [10]

$$J_{TV}(\mathbf{u}) = \|\nabla \mathbf{u}\|_1 = |\mathbf{u}_x| + |\mathbf{u}_y| \tag{3}$$

This work was supported in part by the Macau Science and Technology Development Fund under Grant FDCT/189/2017/A3, and by the Research Committee at University of Macau under Grants MYRG2016-00123-FST and MYRG2018-00136-FST.

where $\nabla = (\frac{\partial}{\partial x}, \frac{\partial}{\partial y})$ denotes the gradient operator and $\nabla \mathbf{u} = (\mathbf{u}_x, \mathbf{u}_y)$. $\mathbf{u}_x$, $\mathbf{u}_y$ denote the gradients of $\mathbf{u}$ in the x and y directions, respectively. $J_{TV}(\mathbf{u})$ is described as the total variation of $\mathbf{u}$.

B. Non-local Total Variation Model

Suppose $\mathbf{u}$ is of size $M \times N$, let $\Omega = \{0, 1, \ldots, M-1\} \times \{0, 1, \ldots, N-1\}$. S_i is a search window with radius s and center pixel i. Then, we can define the non-local partial derivative of $\mathbf{u}$ at i as [11]

$$\nabla_\omega \mathbf{u}(i, j) = \big(\mathbf{u}(i) - \mathbf{u}(j)\big)\sqrt{\omega_{ij}}, j \in S_i \tag{4}$$

where

$$\omega_{ij} = \frac{1}{C(i)} \exp\left(-\frac{||\mathbf{u}(i+\cdot) - \mathbf{u}(j+\cdot)||_a^2}{\sigma_r}\right), j \in S_i \tag{5}$$

and

$$C(i) = \sum_{j \in S_i} \exp\left(-\frac{||\mathbf{u}(i+\cdot) - \mathbf{u}(j+\cdot)||_a^2}{\sigma_r}\right) \tag{6}$$

where a is the Gaussian decay factor. σ_r is smoothing parameter. $\mathbf{u}(i+\cdot)$, $\mathbf{u}(j+\cdot)$ are denoised image patches centered at i and j, respectively.

By replacing the total variation $J_{TV}(\mathbf{u})$ with a non-local total variation $J_{NLTV}(\mathbf{u})$, the NLTV model is defined by [12]

$$\mathbf{u} = \arg\min_{\mathbf{u}} \lambda J_{NLTV}(\mathbf{u}) + \frac{1}{2}\|\mathbf{f} - \mathbf{u}\|_2^2, \tag{7}$$

where

$$\begin{aligned} J_{NLTV}(\mathbf{u}) &= \|\nabla_\omega \mathbf{u}\|_2 \\ &= \sum_{i \in \Omega} \sqrt{\sum_{j \in S_i} \big(\mathbf{u}(i) - \mathbf{u}(j)\big)^2 \omega_{ij}}. \end{aligned} \tag{8}$$

C. Quaternion Representation of the Color Image

Given a quaternion $\dot{q} = a + b\dot{i} + c\dot{j} + d\dot{k}$, it is comprised of one real part and three imaginary parts [13]. a, b, c and d are real numbers, $\dot{i}, \dot{j}$ and $\dot{k}$ are complex operators obeying the rules below

$$\begin{cases} \dot{i}^2 = \dot{j}^2 = \dot{k}^2 = \dot{i}\dot{j}\dot{k} = -1, \\ \dot{i}\dot{j} = \dot{k}, \dot{j}\dot{k} = \dot{i}, \dot{k}\dot{i} = \dot{j}, \\ \dot{j}\dot{i} = -\dot{k}, \dot{k}\dot{j} = -\dot{i}, \dot{i}\dot{k} = -\dot{j}. \end{cases} \tag{9}$$

In addition, we list several important properties of quaternion as followings:

- Conjugate of $\dot{q}$:

$$\bar{\dot{q}} = a - b\dot{i} - c\dot{j} - d\dot{k}. \tag{10}$$

- Modulus of $\dot{q}$:

$$|\dot{q}| = \sqrt{\dot{q}\bar{\dot{q}}} = \sqrt{\bar{\dot{q}}\dot{q}} = \sqrt{a^2 + b^2 + c^2 + d^2}. \tag{11}$$

- Dot product of $\dot{q}$ and $\dot{p} = e + f\dot{i} + g\dot{j} + h\dot{k}$:

$$\dot{q} \cdot \dot{p} = ae + bf + cg + dh. \tag{12}$$

- Cross product of $\dot{q}$ and $\dot{p}$:

$$\dot{q} \times \dot{p} = (ch - dg)\dot{i} + (df - bh)\dot{j} + (bg - cf)\dot{k}. \tag{13}$$

Since a color image in RGB space has three different color channels, i.e. the red, green and blue channels, we can represent a color pixel as a pure quaternion $\dot{q} = r\dot{i} + g\dot{j} + b\dot{k}$, where r, g, b denote the intensity values in the red, green and blue channels, respectively.

Suppose $\dot{\mu}$ is a unit pure quaternion, any unit quaternion $\dot{T}$ related to $\dot{\mu}$ can be expressed as $\dot{T} = |\dot{T}|e^{\dot{\mu}\theta} = \cos\theta + \dot{\mu}\sin\theta$. Then the quaternion unit transforms of a color pixel $\dot{q}$ can be defined as [14]

$$\begin{aligned} \dot{T}\dot{q}\bar{\dot{T}} &= [\cos\theta + \dot{\mu}\sin\theta](r\dot{i} + g\dot{j} + b\dot{k})[\cos\theta - \dot{\mu}\sin\theta] \\ &= \dot{q}^{RGB} + \dot{q}^B + \dot{q}^\Delta, \end{aligned} \tag{14}$$

and

$$\bar{\dot{T}}\dot{q}\dot{T} = \dot{q}^{RGB} + \dot{q}^L - \dot{q}^\Delta, \tag{15}$$

where

$$\begin{cases} \dot{q}^{RGB} &= \dot{q} \cdot \cos 2\theta, \\ \dot{q}^B &= 2\dot{\mu} \cdot (\dot{\mu} \cdot \dot{q}) \cdot \sin^2\theta, \\ \dot{q}^\Delta &= (\dot{\mu} \times \dot{q}) \sin 2\theta. \end{cases} \tag{16}$$

$\dot{q}^B$ and $\dot{q}^\Delta$ are brightness and chromaticity components [15] of pixel $\dot{q}$ in quaternion domain, respectively.

III. Proposed Method

After reviewing two traditional variational models and the quaternion representation of color image, we introduce the coupled quaternion distance to measure the color image patch similarity in the quaternion domain, and then propose a new color image denoising method in quaternion domain, named the Quaternion Non-local Total Variation (QNLTV).

A. Coupled Quaternion Distance

By applying Eqs. (14)-(16) and setting $\theta = \pi/4$ and $\dot{\mu} = \frac{1}{\sqrt{3}}(\dot{i} + \dot{j} + \dot{k})$, we can compute the brightness and chromaticity components of $\dot{\mathbf{u}}$ as

$$\dot{\mathbf{u}}^B = \frac{1}{2}(\dot{T}\dot{\mathbf{u}}\bar{\dot{T}} + \bar{\dot{T}}\dot{\mathbf{u}}\dot{T}), \dot{\mathbf{u}}^\Delta = \frac{1}{2}(\dot{T}\dot{\mathbf{u}}\bar{\dot{T}} - \bar{\dot{T}}\dot{\mathbf{u}}\dot{T}). \tag{17}$$

Then the coupled quaternion distance between two color image patches $\dot{\mathbf{u}}(i+\cdot)$ and $\dot{\mathbf{u}}(j+\cdot)$ is defined as

$$\begin{aligned} &\mathbb{D}\big(\dot{\mathbf{u}}(i+\cdot), \dot{\mathbf{u}}(j+\cdot), \beta\big) \\ &= \|\dot{\mathbf{u}}^B(i+\cdot) - \dot{\mathbf{u}}^B(j+\cdot)\|^\beta \cdot \|\dot{\mathbf{u}}^\Delta(i+\cdot) - \dot{\mathbf{u}}^\Delta(j+\cdot)\|^{1-\beta} \end{aligned} \tag{18}$$

where $\beta \in [0, 1]$ is a trade-off parameter.

B. QNLTV

In this subsection, we propose the Quaternion Non-local Total Variation (QNLTV) for color image denoising in the quaternion domain. Its quaternion optimization model is defined by

$$\dot{\mathbf{u}} = \arg\min_{\dot{\mathbf{u}}} J_{QNLTV}(\dot{\mathbf{u}}) + \frac{1}{2}\|\dot{\mathbf{f}} - \dot{\mathbf{u}}\|^2, \tag{19}$$

where

$$J_{QNLTV}(\dot{\mathbf{u}}) \quad = \lambda_1 \|\nabla_\omega \dot{\mathbf{u}}^B\| + \lambda_2 \|\nabla_v \dot{\mathbf{u}}^\Delta\|. \tag{20}$$

where λ_1 and λ_2 are penalty parameters.

Since we use Eq. (17) to decompose the variable $\dot{\mathbf{u}}$ into two components $\dot{\mathbf{u}}^B$ and $\dot{\mathbf{u}}^\Delta$, the original quaternion optimization model Eq. (19) can be separated into two quaternion subproblems

$$\dot{\mathbf{u}}^B = \arg\min_{\dot{\mathbf{u}}^B} \lambda_1 \|\nabla_\omega \dot{\mathbf{u}}^B\| + \frac{1}{2}\|\dot{\mathbf{f}} - \bar{\dot{T}}(\dot{\mathbf{u}}^B + \dot{\mathbf{u}}^\Delta)\dot{T}\|^2, \tag{21}$$

$$\dot{\mathbf{u}}^\Delta = \arg\min_{\dot{\mathbf{u}}^\Delta} \lambda_2 \|\nabla_v \dot{\mathbf{u}}^\Delta\| + \frac{1}{2}\|\dot{\mathbf{f}} - \bar{\dot{T}}(\dot{\mathbf{u}}^B + \dot{\mathbf{u}}^\Delta)\dot{T}\|^2. \tag{22}$$

To solve the quaternion optimization problems in Eqs. (21) and (22), we propose a quaternion split Bregman method. Firstly, We replace $\nabla_\omega \dot{\mathbf{u}}^B$ with $\dot{\mathbf{d}}^B$ and introduce an auxiliary variable $\dot{\mathbf{b}}^B$, and thus the solution of Eq. (21) is equivalent to solve the following quaternion optimization problem

$$\begin{aligned}\{\dot{\mathbf{u}}^B, \dot{\mathbf{d}}^B\} = \arg\min_{\dot{\mathbf{u}}^B, \dot{\mathbf{d}}^B} \lambda_1 \|\dot{\mathbf{d}}^B\| + \frac{1}{2}\|f - \bar{\dot{T}}(\dot{\mathbf{u}}^B + \dot{\mathbf{u}}^\Delta)\dot{T}\|^2 \\ + \frac{\alpha_1}{2}\|\dot{\mathbf{d}}^B - \nabla_\omega \dot{\mathbf{u}}^B - \dot{\mathbf{b}}^B\|^2,\end{aligned} \tag{23}$$

where

$$\dot{\mathbf{b}}^B := \dot{\mathbf{b}}^B + \nabla_\omega \dot{\mathbf{u}}^B - \dot{\mathbf{d}}^B. \tag{24}$$

Next, we optimize $\dot{\mathbf{u}}^B$ and $\dot{\mathbf{d}}^B$ by alternatively solving Eqs. (25) and (26)

$$\begin{aligned}\dot{\mathbf{u}}^B = \arg\min_{\dot{\mathbf{u}}^B} \frac{1}{2}\|f - \bar{\dot{T}}(\dot{\mathbf{u}}^B + \dot{\mathbf{u}}^\Delta)\dot{T}\|^2 \\ + \frac{\alpha_1}{2}\|\dot{\mathbf{d}}^B - \nabla_\omega \dot{\mathbf{u}}^B - \dot{\mathbf{b}}^B\|^2,\end{aligned} \tag{25}$$

$$\dot{\mathbf{d}}^B = \arg\min_{\dot{\mathbf{d}}^B} \lambda_1 \|\dot{\mathbf{d}}^B\| + \frac{\alpha_1}{2}\|\dot{\mathbf{d}}^B - \nabla_\omega \dot{\mathbf{u}}^B - \dot{\mathbf{b}}^B\|^2. \tag{26}$$

To solve $\dot{\mathbf{u}}^B$, we calculate weight ω_{ij} $(j \in S_i)$ by Eq. (27), and then derive the Euler-Lagrange equation from Eq. (25) to obtain Eq. (28):

$$\omega_{ij}^{(t+1)} = \frac{1}{C_\omega(i)} \exp\left(-\frac{\mathbb{D}\big(\dot{\mathbf{u}}^{(t)}(i+\cdot), \dot{\mathbf{u}}^{(t)}(j+\cdot), \beta_1\big)}{\sigma_r^B}\right), \tag{27}$$

$$\dot{\mathbf{u}}^{B^{(t+1)}} = \frac{\dot{\mathbf{u}}^{\Delta^{(t)}} - \dot{T}\dot{\mathbf{f}}\bar{\dot{T}} + \alpha_1 \nabla_\omega (\dot{\mathbf{b}}^{B^{(t)}} - \dot{\mathbf{d}}^{B^{(t)}})}{1 - \alpha_1 \Delta_\omega}. \tag{28}$$

where $\sum_{j \in S_i} \omega_{ij} = 1$ and Δ_ω is the graph Laplacian operator [16]. To solve $\dot{\mathbf{d}}^B$, we apply the soft-shrinkage operator [3] and obtain the equation below

$$\dot{\mathbf{d}}^{B^{(t+1)}} = shrink(\nabla_\omega \dot{\mathbf{u}}^{B^{(t+1)}} + \dot{\mathbf{b}}^{B^{(t)}}, \frac{\lambda_1}{\alpha_1}), \tag{29}$$

where

$$\dot{\mathbf{b}}^{B^{(t+1)}} = \dot{\mathbf{b}}^{B^{(t)}} + \nabla_\omega \dot{\mathbf{u}}^{B^{(t+1)}} - \dot{\mathbf{d}}^{B^{(t+1)}}. \tag{30}$$

Similarly, we can calculate v_{ij} $(j \in S_i)$, $\dot{\mathbf{u}}^\Delta$, $\dot{\mathbf{d}}^\Delta$ and $\dot{\mathbf{b}}^\Delta$ by the following updating processes

$$v_{ij}^{(t+1)} = \frac{1}{C_\Delta(i)} \exp\left(-\frac{\mathbb{D}\big(\dot{\mathbf{u}}^{(t)}(i+\cdot), \dot{\mathbf{u}}^{(t)}(j+\cdot), \beta_2\big)}{\sigma_r^\Delta}\right), \tag{31}$$

$$\dot{\mathbf{u}}^{\Delta^{(t+1)}} = \frac{\dot{\mathbf{u}}^{B^{(t+1)}} - \dot{T}\dot{\mathbf{f}}\bar{\dot{T}} + \alpha_2 \nabla_v (\dot{\mathbf{b}}^{\Delta^{(t)}} - \dot{\mathbf{d}}^{\Delta^{(t)}})}{1 - \alpha_2 \Delta_v}, \tag{32}$$

$$\dot{\mathbf{d}}^{\Delta^{(t+1)}} = shrink(\nabla_v \dot{\mathbf{u}}^{\Delta^{(t+1)}} + \dot{\mathbf{b}}^{\Delta^{(t)}}, \frac{\lambda_2}{\alpha_2}), \tag{33}$$

$$\dot{\mathbf{b}}^{\Delta^{(t+1)}} = \dot{\mathbf{b}}^{\Delta^{(t)}} + \nabla_v \dot{\mathbf{u}}^{\Delta^{(t+1)}} - \dot{\mathbf{d}}^{\Delta^{(t+1)}}. \tag{34}$$

where $\sum_{j \in S_i} v_{ij} = 1$.

The processes of QNLTV are shown in Algorithm 1.

Algorithm 1 QNLTV

Input: Noisy image f; Parameters $\dot{T}$, λ_1, λ_2, α_1, α_2, β, σ_r^B, σ_r^Δ,a;

Output: Denoised image $\dot{\mathbf{u}}$;

Initialize $\dot{\mathbf{u}}^{(0)} = f$, $\dot{\mathbf{d}}^{B^{(0)}} = \dot{\mathbf{b}}^{B^{(0)}} = \dot{\mathbf{d}}^{\Delta^{(0)}} = \dot{\mathbf{b}}^{\Delta^{(0)}} = 0$ and $t = 0$;
while not satisfy the termination **do**
  Extract $\dot{\mathbf{u}}^{B^{(t)}}$ and $\dot{\mathbf{u}}^{\Delta^{(t)}}$ from $\dot{\mathbf{u}}^{(t)}$ by Eq. (17);
  Calculate $\omega_{ij}^{(t+1)}$ $(j \in S_i)$ by Eq. (27);
  Update $\dot{\mathbf{u}}^{B^{(t+1)}}$ by Eq. (28).
  Update $\dot{\mathbf{d}}^{B^{(t+1)}}$ by Eq. (29).
  Update $\dot{\mathbf{b}}^{B^{(t+1)}}$ by Eq. (30).
  Calculate $v_{ij}^{(t+1)}$ $(j \in S_i)$ by Eq. (31);
  Update $\dot{\mathbf{u}}^{\Delta^{(t+1)}}$ by Eq. (32).
  Update $\dot{\mathbf{d}}^{\Delta^{(t+1)}}$ by Eq. (33).
  Update $\dot{\mathbf{b}}^{\Delta^{(t+1)}}$ by Eq. (34).
  Update $\dot{\mathbf{u}}^{(t+1)} = \bar{\dot{T}}(\dot{\mathbf{u}}^{B^{(t+1)}} + \dot{\mathbf{u}}^{\Delta^{(t+1)}})\dot{T}$
  $t = t + 1$;
end while
return $\dot{\mathbf{u}}$

IV. Experiments

We compare the denoising performance of QNLTV with that of eight existing color image denoising methods. They are NLM [6], TV [2], TV-AFT[1] [4], VIRN [5], SB-ATV [3], SB-ITV [3], NLTV [12] and NLGRTV [9]. All simulations are implemented in Matlab with forty test color images of size about 256×256. We utilize signal-to-noise ratio (SNR), structural similarity index (SSIM) [17] and method noise to evaluate the denoising performance of each method.

Table I presents the SNR and SSIM values of four test images at noise levels $\sigma = 10, 20, \cdots, 100$. For easy comparison, we list the SNR and SSIM of corresponding noisy images for each test image. The best results are highlighted in blue. Obviously, QNLTV performs the best in all situations.

[1]The TV model with adaptive fidelity term in [4]

TABLE I

SNR AND SSIM RESULTS OF QNLTV AND OTHER METHODS AT NOISE LEVELS $\sigma = 10, 20, \cdots, 100$.

Image	Method\σ	SNR(dB) 10	20	30	40	50	60	70	80	90	100	SSIM(%) 10	20	30	40	50	60	70	80	90	100
	QNLTV	**26.97**	**23.52**	**21.63**	**20.20**	**18.94**	**18.03**	**17.17**	**16.18**	**15.65**	**15.19**	**95.85**	**92.68**	**89.89**	**87.04**	**83.91**	**80.57**	**78.04**	**73.74**	**70.88**	**68.37**
	NLM [6]	26.25	22.38	19.81	18.04	16.74	15.71	14.94	14.33	13.91	13.54	95.37	91.15	86.80	82.85	79.22	76.10	73.42	70.92	68.65	66.65
	NLTV [8]	26.11	22.70	20.52	18.87	17.55	16.61	15.82	15.14	14.68	14.21	95.18	91.47	87.32	82.72	77.96	73.61	69.46	65.85	62.92	59.82
	NLGRTV [9]	24.82	20.52	17.62	16.23	15.45	15.00	14.72	14.40	14.08	13.81	94.37	88.25	82.84	77.77	73.95	70.66	68.44	65.43	64.06	61.84
	TV [2]	23.68	19.76	18.06	16.90	16.13	15.55	14.98	14.63	14.29	14.01	92.78	86.68	82.10	78.44	74.65	72.30	70.41	68.44	66.35	64.53
lighthouse	TV-AFT	25.10	21.35	19.23	17.83	16.80	16.17	15.59	15.10	14.73	14.36	94.96	90.68	86.25	82.09	78.53	75.89	73.53	71.46	68.74	67.40
	VIRN	24.11	21.14	18.88	17.98	16.79	16.41	15.73	15.30	14.84	14.18	93.86	89.08	83.99	80.01	76.87	73.29	70.16	67.07	63.44	57.89
	SB-ATV [3]	25.23	21.07	18.42	17.47	16.32	15.80	15.35	14.90	14.58	14.30	94.63	89.33	84.41	80.49	77.21	74.51	72.12	69.97	68.14	66.80
	SB-ITV [3]	25.23	21.06	18.67	17.17	16.31	15.75	15.26	14.77	14.50	14.24	94.26	88.28	84.18	80.20	76.82	74.13	71.94	70.11	68.16	66.67
	noisy	22.69	16.68	13.19	10.68	8.74	7.17	5.83	4.67	3.66	2.72	84.83	66.94	53.70	43.62	35.81	29.82	24.98	21.17	18.15	15.59
	QNLTV	**27.30**	**24.36**	**22.55**	**21.19**	**20.16**	**19.19**	**18.44**	**17.79**	**17.28**	**16.70**	**99.08**	**98.32**	**97.54**	**96.69**	**95.84**	**94.93**	**94.01**	**93.07**	**92.21**	**91.39**
	NLM [6]	25.91	22.19	19.59	17.90	16.58	15.57	14.69	14.02	13.49	13.04	98.85	97.47	95.70	93.85	91.93	90.18	88.45	86.89	85.62	84.57
	NLTV [8]	26.66	23.43	21.45	19.92	18.77	17.78	17.02	16.40	15.87	15.33	98.96	97.94	96.80	95.52	94.21	92.89	91.58	90.39	89.20	88.18
	NLGRTV [9]	26.17	22.36	20.36	19.27	18.47	17.77	17.21	16.76	16.38	15.85	98.85	97.36	95.94	94.89	93.95	93.05	92.08	91.25	90.55	89.60
	TV [2]	25.96	22.81	21.11	19.89	18.91	18.07	17.35	16.84	16.37	15.94	98.78	97.60	96.52	95.50	94.47	93.41	92.35	91.51	90.53	89.85
peppers	TV-AFT	26.66	23.45	21.54	20.18	19.22	18.41	17.59	17.14	16.72	16.08	98.97	97.94	96.86	95.77	94.85	93.90	92.71	92.04	91.26	90.28
	VIRN	26.31	23.26	21.28	20.04	19.22	18.36	17.63	17.01	16.50	15.37	98.89	97.81	96.62	95.53	94.73	93.66	92.60	91.50	90.43	88.08
	SB-ATV [3]	26.56	23.11	21.10	19.92	18.96	18.17	17.52	17.06	16.64	16.14	98.93	97.73	96.48	95.45	94.45	93.50	92.50	91.76	91.00	90.24
	SB-ITV [3]	26.57	23.02	21.30	20.02	19.09	18.29	17.62	17.12	16.72	16.23	98.93	97.67	96.61	95.55	94.61	93.64	92.64	91.87	91.12	90.41
	noisy	22.20	16.19	12.66	10.17	8.24	6.64	5.30	4.14	3.11	2.19	97.10	89.76	80.31	70.61	61.63	53.51	46.51	40.45	35.25	31.04
	QNLTV	**29.60**	**27.21**	**25.47**	**24.22**	**22.98**	**22.07**	**21.23**	**20.22**	**19.39**	**18.85**	**99.17**	**98.62**	**98.08**	**97.35**	**96.50**	**95.71**	**94.86**	**93.57**	**92.45**	**92.07**
	NLM [6]	28.88	25.71	23.76	21.87	20.04	18.74	17.77	16.85	16.21	15.68	99.08	98.05	97.15	95.72	93.86	92.40	90.90	89.56	88.09	87.33
	NLTV [8]	29.42	26.57	24.57	22.82	21.43	20.31	19.39	18.58	17.87	17.36	99.14	98.36	97.50	96.24	94.97	93.71	92.38	91.06	89.68	89.01
	NLGRTV [9]	28.33	24.67	23.26	21.99	20.87	20.09	19.37	18.62	18.24	17.75	98.82	97.42	96.83	95.76	94.63	93.72	92.82	91.59	90.95	90.50
	TV [2]	27.72	25.48	23.95	22.83	21.45	20.68	20.09	19.24	18.70	18.22	98.61	97.74	97.17	96.39	95.16	94.52	93.88	92.80	91.74	91.19
splash	TV-AFT	29.18	26.54	24.77	23.30	22.12	21.25	20.53	19.74	19.17	18.78	99.08	98.34	97.72	96.75	95.91	95.12	94.38	93.37	92.40	92.00
	VIRN	28.16	25.88	23.70	22.19	21.51	20.37	19.55	18.60	17.84	16.50	98.74	98.00	96.95	95.74	95.21	93.84	92.89	91.46	90.11	87.86
	SB-ATV [3]	29.19	26.11	24.49	22.92	21.89	20.96	20.20	19.52	18.96	18.56	99.02	98.09	97.55	96.43	95.72	94.76	93.95	93.07	92.04	91.72
	SB-ITV [3]	28.60	25.24	24.03	22.89	21.72	20.80	20.12	19.50	18.92	18.54	98.86	97.62	97.19	96.42	95.51	94.51	93.80	93.04	91.97	91.68
	noisy	22.35	16.34	12.83	10.32	8.38	6.80	5.47	4.28	3.24	2.36	95.63	87.51	78.86	70.46	62.64	55.59	49.47	43.84	38.95	34.99
	QNLTV	**26.84**	**23.06**	**20.94**	**19.33**	**18.09**	**17.07**	**16.27**	**15.77**	**15.20**	**14.78**	**97.87**	**95.32**	**92.37**	**88.77**	**84.91**	**81.14**	**77.04**	**74.66**	**71.49**	**69.10**
	NLM [6]	25.13	20.56	17.84	16.16	14.94	14.22	13.72	13.23	12.86	12.64	97.04	91.94	86.38	80.45	75.62	72.65	69.81	67.50	65.58	64.49
	NLTV [8]	25.47	21.40	19.04	17.58	16.59	15.77	15.16	14.62	14.05	13.74	97.08	93.10	87.85	82.81	78.37	74.45	70.51	67.71	64.14	62.29
	NLGRTV [9]	23.55	19.52	17.09	16.24	15.73	15.33	15.03	14.68	14.32	14.07	94.98	88.19	80.08	76.13	73.54	71.48	69.08	66.72	65.19	63.98
	TV [2]	24.26	20.67	18.59	17.15	16.25	15.48	14.92	14.55	14.20	13.94	95.46	91.23	86.27	81.24	77.06	73.03	69.87	67.90	65.98	65.05
windows	TV-AFT	24.91	21.17	19.01	17.60	16.66	15.92	15.37	14.93	14.45	14.25	96.65	92.56	87.84	83.49	79.83	76.51	72.86	71.17	68.15	66.96
	VIRN	24.43	21.13	19.01	17.93	16.90	16.25	15.68	15.17	14.58	13.75	96.03	91.67	86.76	82.73	79.18	75.66	72.33	69.70	66.13	60.88
	SB-ATV [3]	24.89	20.92	18.45	17.42	16.32	15.70	15.28	14.90	14.48	14.29	96.48	91.81	86.03	82.10	77.48	74.55	71.76	69.88	67.70	66.85
	SB-ITV [3]	24.78	20.86	18.73	17.28	16.41	15.75	15.30	14.88	14.51	14.32	96.05	91.01	86.39	81.44	77.59	74.49	71.74	69.92	67.89	67.00
	noisy	20.78	14.80	11.26	8.74	6.82	5.23	3.88	2.73	1.68	0.79	87.16	67.64	52.02	40.63	32.22	26.13	21.28	17.68	14.85	12.73

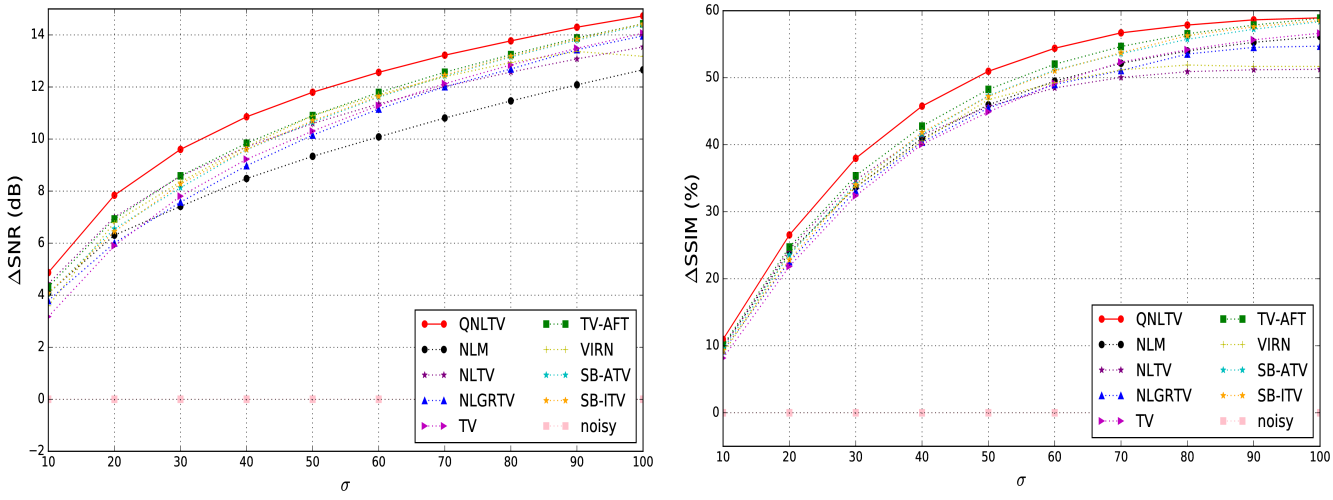

(a) (b)

Fig. 1. Average gains of (a) SNR and (b) SSIM over corresponding noisy images.

Fig. 1 shows the average gains of SNR and SSIM over the corresponding noisy images as noise level σ ranges from 10 to 100. In terms of SNR (Fig. 1(a)), QNLTV can improve the average SNR value by 5.0 dB at $\sigma = 10$ and about 14.8 dB at $\sigma = 100$. As can be seen, QNLTV is about 1.0 dB higher than TV-AFT and 1.5 dB higher than NLTV when σ ranges from 20 to 80. Considering the SSIM index (Fig. 1(b)), the average ΔSSIM value of QNLTV increases from 11% to 59%. Compared with TV, QNLTV achieves an obvious improvement by about 5% as noise level $\sigma \geq 20$. When noise level $20 < \sigma < 90$, QNLTV surpasses TV-AFT by about 3%.

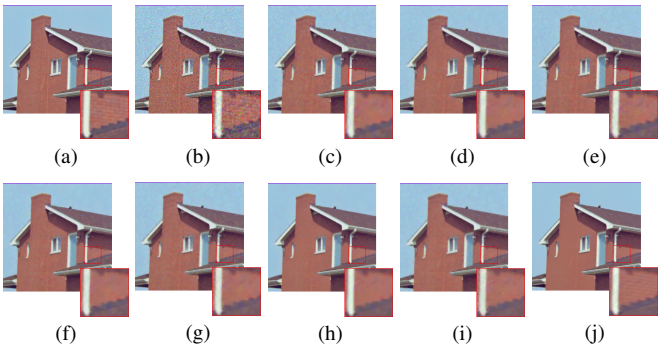

Fig. 2. Denoised results of the *house* image with noise $\sigma = 20$: (a) clean image; (b) noisy image; (c) TV; (d) SB-ATV; (e) SB-ITV; (f) TV-AFT; (g) VIRN; (h) NLTV; (i) NLGRTV; (j) QNLTV.

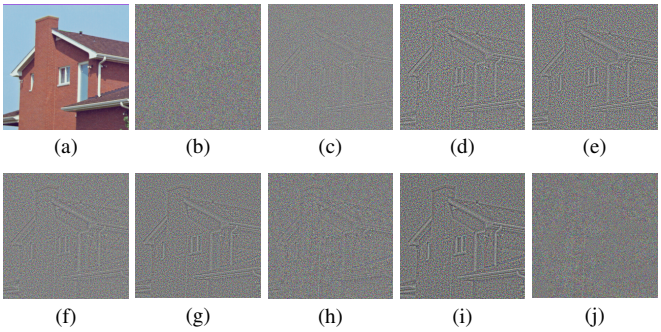

Fig. 3. Method noises of the *house* image with noise $\sigma = 20$: (a) clean image; (b) noise; (c) TV; (d) SB-ATV; (e) SB-ITV; (f) TV-AFT; (g) VIRN; (h) NLTV; (i) NLGRTV; (j) QNLTV.

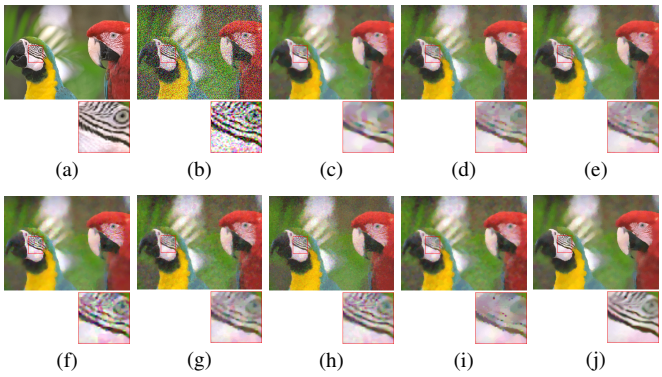

Fig. 4. Denoised results of the *parrots* image with noise $\sigma = 70$: (a) clean image; (b) noisy image; (c) TV; (d) SB-ATV; (e) SB-ITV; (f) TV-AFT; (g) VIRN; (h) NLTV; (i) NLGRTV; (j) QNLTV.

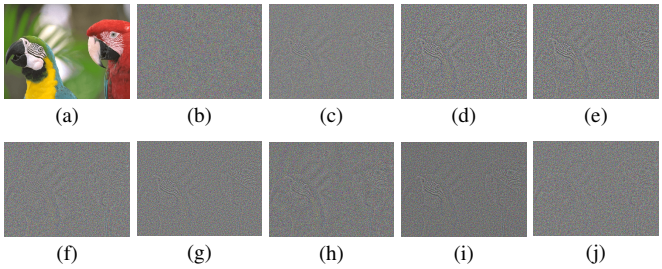

Fig. 5. Method noises of the *parrots* image with noise $\sigma = 70$: (a) clean image; (b) noise; (c) TV; (d) SB-ATV; (e) SB-ITV; (f) TV-AFT; (g) VIRN; (h) NLTV; (i) NLGRTV; (j) QNLTV.

Fig. 2 presents the denoised results of the *house* image at noise level $\sigma = 20$. In the denoised results of TV and SB-ITV, there are some noise residuals. NLGRTV over-smooths the image and leaves many noticeable spots. SB-ATV, TV-AFT, VIRN and NLTV perform well in noise removal but lose fine structure information. According to the zoom-in parts, we observe that QNLTV can greatly suppress noise and preserve the textures of the house. However, other competing methods fail to keep the details. The corresponding method noise results of the *house* image are shown in Fig. 3. For easy comparing and analyzing, we show the related clean and noise images in Figs. 3(a) and 3(b), respectively. As can be seen, we can recognize more or less the outline of the house in the method noise results of the competing denoising methods. However, there is almost no loss of structure information after denoising by QNLTV.

Another case of denoising under heavy noise ($\sigma = 70$) is shown in Figs. 4 and 5. As can be seen from the zoom-in parts, QNLTV keeps more distinct and clear textures of the parrot than other methods. TV, SB-ATV, SB-ITV and NLGRTV casue blur in the textural areas. VIRN and NLTV preserve many details, but introduce serious artifacts in the smooth areas. Although TV-AFT shows relatively strong capability of preserving details, there is obvious color blending effect occurred in the regions near the edges. Fig. 5 presents the related method noise results of the *parrots* image. We can still identify the textures around the eyes of the parrots in Figs. 5(c)-(i). Compared with the competing methods, the method noise result of QNLTV contains much less image information.

V. Conclusion

In this paper, we utilized the quaternion representation of color image to propose the Quaternion Non-local Total Variation (QNLTV) model for color image denoising in the quaternion domain. Applying the unit quaternion transform, we first splitted the original color image into a brightness component and a chromaticity component in quaternion domain, and then introduced the coupled quaternion distance to measure the similarity between two color image patches in quaternion domain. Based on the decomposition of the quaternion representation of the color image, the original QNLTV model was separated into two quaternion optimization models to alternatively optimize $\dot{\mathbf{u}}^B$ and $\dot{\mathbf{u}}^\Delta$. Unlike many TV-based denoising methods using only color intensity for denoising, QNLTV can take advantages of both brightness and chromaticity information to denoise a color image in the quaternion domain. Simulation results showed that QNLTV achieves much better denoising performance than other competing variational methods in terms of both quantitative and visual comparisons.

REFERENCES

[1] Qiang Chen, Philippe Montesinos, Quan Sen Sun, Peng Ann Heng, and De Shen Xia, "Adaptive total variation denoising based on difference curvature," *Image and Vision Computing*, vol. 28, no. 3, pp. 298–306, 2010.

[2] Leonid I. Rudin, Stanley Osher, and Emad Fatemi, "Nonlinear total variation based noise removal algorithms," *Physical D*, vol. 60, no. 1-4, pp. 259–268, 1992.

[3] Tom Goldstein and Stanley Osher, "The split bregman method for l1-regularized problems," *SIAM Journal on Imaging Sciences*, vol. 2, no. 2, pp. 323–343, Apr. 2009.

[4] Guy Gilboa, Yehoshua Zeevi, and Nir Sochen, "Texture preserving variational denoising using an adaptive fidelity term," *Proc VLSM Nice, France 1*, 01 2003.

[5] Paul Rodr´ıguez and Brendt Wohlberg, "A generalized vector-valued total variation algorithm," in *Proceedings of the 16th IEEE International Conference on Image Processing*, ser. ICIP'09, 2009, pp. 1301–1304.

[6] Antoni Buades, Bartomeu Coll, and Jean-Michel Morel, "A non-local algorithm for image denoising," in *2005 IEEE Computer Society Conference on Computer Vision and Pattern Recognition (CVPR'05)*, vol. 2, June 2005, pp. 60–65.

[7] ——, "A review of image denoising algorithms, with a new one," *SIAM Journal on Multiscale Modeling and Simulation*, vol. 4, no. 2, pp. 490–530, 2005.

[8] Guy Gilboa and Stanley Osher, "Nonlocal linear image regularization and supervised segmentation," *Multiscale Modeling & Simulation*, vol. 6, no. 2, pp. 595–630, 2007.

[9] Qiegen Liu, Biao Xiong, and Minghui Zhang, "Adaptive sparse norm and nonlocal total variation methods for image smoothing," *Mathematical Problems in Engineering*, 12 2014.

[10] Jie Yan and Wu-Sheng Lu, "Image denoising by generalized total variation regularization and least squares fidelity," *Multidimensional Systems and Signal Processing*, vol. 26, no. 1, pp. 243–266, 2015.

[11] Yifei Lou, Xiaoqun Zhang, Stanley Osher, and Andrea Bertozzi, "Image recovery via nonlocal operators," *Journal of Scientific Computing*, vol. 42, no. 2, pp. 185–197, 2010.

[12] Guy Gilboa and Stanley Osher, "Nonlocal operators with applications to image processing," *Multiscale Modeling and Simulation*, vol. 7, no. 3, pp. 1005–1028, 2008.

[13] William Rowan Hamilton, "Scientific books: Elements of quaternions," vol. 14, pp. 65–66, 1901.

[14] Canhui Cai and S. K. Mitra, "A normalized color difference edge detector based on quaternion representation," in *Proceedings 2000 International Conference on Image Processing*, vol. 2, 2000, pp. 816–819 vol.2.

[15] Konstantinos N. Plataniotis and Anastasios N. Venetsanopoulos, "Color image processing and applications," *Springer-Verlag New York, Inc.*, 2000.

[16] Xiaoqun Zhang, Martin Burger, Xavier Bresson, and Stanley Osher, "Bregmanized nonlocal regularization for deconvolution and sparse reconstruction," *SIAM Journal on Imaging Sciences*, vol. 3, no. 3, pp. 253–276, 2010.

[17] Zhou Wang, Alan Conrad Bovik, Hamid Rahim Sheikh, and Eero P. Simoncelli, "Image quality assessment: from error visibility to structural similarity," *IEEE Transactions on Image Processing*, vol. 13, no. 4, pp. 600–612, 2004.